

Fig. 5. Combined heat loss characteristics for wire upstream 0.002 in. at $\Delta T = 100^\circ\text{C}$, film at $\Delta T = 275^\circ\text{C}$.

the film, the wire is uninfluenced by the film, and the non-interfering behavior shown in Figs. 1–3 is recovered. Again this is undesirable.

To indicate the sort of sensitivity that can be obtained by the configuration under discussion we show in Fig. 5 the performance of a probe with the upstream wire separated by 0.002 in. from the film and operated at 100°C overheat. The dramatic increase in sensitivity to concentration is apparent from a comparison of Figs. 3 and 5. We add to the lines of constant concentration in Fig. 5 isovelocity lines in order to indicate the concentration-velocity range for which there can be realized superior sensitivity. We find from Fig. 5 that for a velocity range with a lower end of $u = 25$ cm/sec and an upper end depending on concentration, $E_w^2 \approx \bar{a}(c) + \bar{b}E_f^2$ where \bar{b} is constant so that a simple means for obtaining c is evident. In addition the film is found to be unaffected by the wire so that Fig. 2 still applies. Thus we can readily invert from voltage pairs to u and c pairs.

Concluding Remarks

In conclusion we note that a probe similar to that resulting in the data of Fig. 5 but with greater sensitivity to concentration at high velocities and low concentrations can be obtained by increasing the film temperature and that a relatively cool "X-wire" in the thermal field of the film would appear to provide a means for measuring u , v , and c . We also note that other interfering configurations can be considered, e.g., a relatively cool wire downstream of a film, but the configuration leading to the results of Fig. 5, although perhaps not unique, does have the great virtue of having nearly orthogonal contours of constant concentration and constant velocity. Other interfering sensors we have tried lead to corresponding contours which are highly skewed and thus to degraded accuracy in separating c and u .

References

- Corrsin, S., "Extended Applications of the Hot-Wire Anemometer," TN 1864, 1949, NACA.
- Tombach, I. H., "Velocity Measurements with a New Probe in Inhomogeneous Turbulent Jets," thesis, California Institute of Technology, 1969.
- Aihara, Y., Kassoy, D. R., and Libby, P. A., "Heat Transfer from Circular Cylinders at Low Reynolds Numbers. II Experimental Results and Comparison with Theory," *The Physics of Fluids*, Vol. 10, No. 10, May 1967, pp. 947–952.
- Baccaglioni, G., Kassoy, D. R., and Libby, P. A., "Heat Transfer in Nitrogen-Helium and Nitrogen-Neon Mixtures," *The Physics of Fluids*, Vol. 12, 1969, pp. 1378–1381.

Effect of Spin on the Velocity of a Re-Entry Body

ALI HASAN NAYFEH*

Aerotherm Corporation, Mountain View, Calif.

1. Introduction

THE purpose of the present Note is to derive an approximate expression for the velocity of a rolling re-entry body as a function of roll, pitch, and yaw rates as well as the re-entry angle of attack. The present analysis is an extension of the analysis of Ref. 1.

In the analysis, the rotational motion is decoupled from the translational motion. A closed form expression for the angle of attack is given. This expression for the angle of attack is then used to calculate the drag of the body, which is used in turn to determine the variation of the velocity with altitude. The results of the analysis are in good agreement with six-degree-of-freedom numerical computations.

2. Angle of Attack

A number of investigators^{2–7} determined the angle of attack allowing for variable velocity, dynamic pressure, and aerodynamic derivatives. References 6 and 7 allowed also for small mass and aerodynamic asymmetries as well as roll accelerations. For a constant roll rate, and for an axisymmetric body, the complex angle of attack $\delta = \beta + i\alpha$ can be written as⁶

$$\delta = [R_1/(V\omega)^{1/2}]e^{-\Lambda_1 e^{i\Omega_1}} + [R_2/(V\omega)^{1/2}]e^{-\Lambda_2 e^{i\Omega_2}} \quad (1)$$

$$\Omega_{1,2} = \int_0^t \left(\frac{\omega \pm pI_x}{2I} \right) dt \quad (2)$$

$$\Lambda_{1,2} = \int_0^t (\lambda \pm \Delta\lambda) dt \quad (3)$$

$$\omega = -[(C_{m\alpha}AdV^2/2I)\rho + (I_x p/2I)^2]^{1/2}$$

$$\lambda = -(C_{N\alpha}/m - C_{mq}d^2/2I)(AV/4)\rho$$

$$\Delta\lambda = -(C_{N\alpha}/m + C_{mq}d^2/2I)AVI_x p/8\omega I \rho$$

where m is the body mass, A area, d diameter, I_x roll moment of inertia, I transverse moment of inertia, V velocity, $C_{N\alpha}$ normal force derivative, $C_{m\alpha}$ pitching moment coefficient, and C_{mq} is pitching or yawing damping coefficient. In this solution, the angle of attack is assumed small, but the velocity, dynamic pressure, and aerodynamic derivatives are assumed to be slowly varying in comparison with the angle-of-attack oscillations. The complex constants of integration R_1 and R_2 are determined from the re-entry initial conditions (denoted by e); that is

$$R_1 = (\delta_e - I\zeta_e/I_x p)(V_e\omega_e)^{1/2} \quad (4)$$

$$R_2 = (I\zeta_e/I_x p)(V_e\omega_e)^{1/2} \quad (5)$$

where $\zeta_e = q_e + ir_e$ with q_e and r_e the initial pitch and yaw rates.

For a high-performance re-entry vehicle, the velocity and trajectory path angle change appreciably only at the lower altitudes where the angles of attack have converged. Thus, the velocity and path angle in Eqs. (1–3) will be assumed constant. In addition, the aerodynamic derivatives are assumed constant. Assuming an exponential atmosphere;

Received December 22, 1969. Work done under contract for Sandia Corporation, Albuquerque, N. Mex.

* Manager, Mathematical Physics Department. Member AIAA.

i.e.,

$$\rho = \rho_0 e^{-h/k} \quad (6)$$

leads to

$$dt = (k/\rho V \sin \gamma) d\rho \quad (7)$$

With these assumptions, Ω_i and Λ_i become

$$\Omega_1 = \frac{I_x k}{IV_e \sin \gamma} \left[-p \log \frac{\xi + ap}{\xi_e + ap} + \frac{\xi - \xi_e}{a} \right] \quad (8)$$

$$\Omega_2 = \frac{I_x k}{IV_e \sin \gamma} \left[-p \log \frac{\xi + ap}{\xi_e + ap} + \frac{\xi - \xi_e}{a} + p \log \frac{\rho}{\rho_e} \right] \quad (9)$$

$$\Lambda_{1,2} = b_1(\rho - \rho_e) \pm 2b_2 ap(\xi - \xi_e) \quad (10)$$

where

$$b_{1,2} = (\pm C_{N\alpha}/m - C_{mq}d^2/2I)Ak/4 \sin \gamma$$

$$a = I_x/(-2C_{m\alpha}AdIV_e^2)^{1/2}, \quad \xi = (\rho + a^2p^2)^{1/2}$$

Figure 1 shows good agreement between the angle-of-attack envelope predicted from the present analysis with that calculated using a six-degree-of-freedom computer program for $p = 0, 50, 250$ rad/sec. In the calculations, $V_e = 20,000$ fps, $\gamma = 30^\circ$, $|\delta| = 36^\circ$, $C_{N\alpha} = 2.58/\text{rad}$, $C_{m\alpha} = -0.344/\text{rad}$, $C_{mq} = 0$, $\rho_0 = 0.00247$ slug/ft³, $k = 23,260$ ft. The rest of the body parameters are the same as those used in Ref. 8.

3. Velocity

In determining the velocity history, the drag coefficient is assumed to be

$$C_D = C_{D0} + C_{N\alpha}|\delta|^2 \quad (11)$$

where C_{D0} is the drag coefficient at zero angle of attack. The drag coefficient is composed of a slowly altitude varying term, and a fast varying oscillatory term. The effect of the oscillatory term can be neglected because its effect approxi-

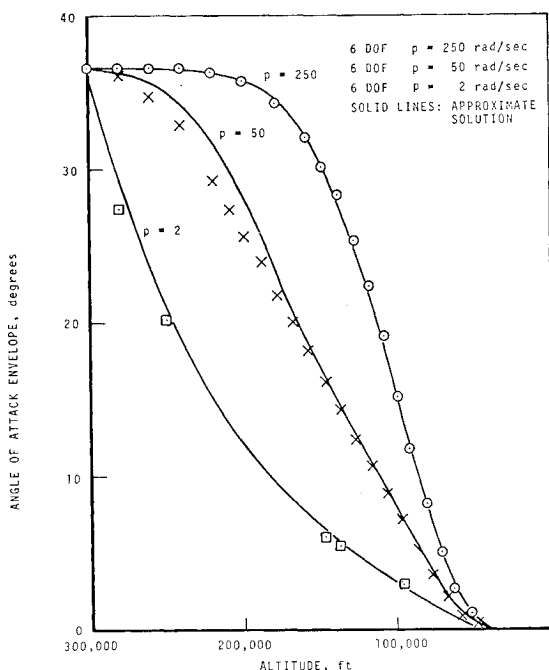


Fig. 1 Comparison of the analytic result with 6-DOF computations for the angle-of-attack envelope.

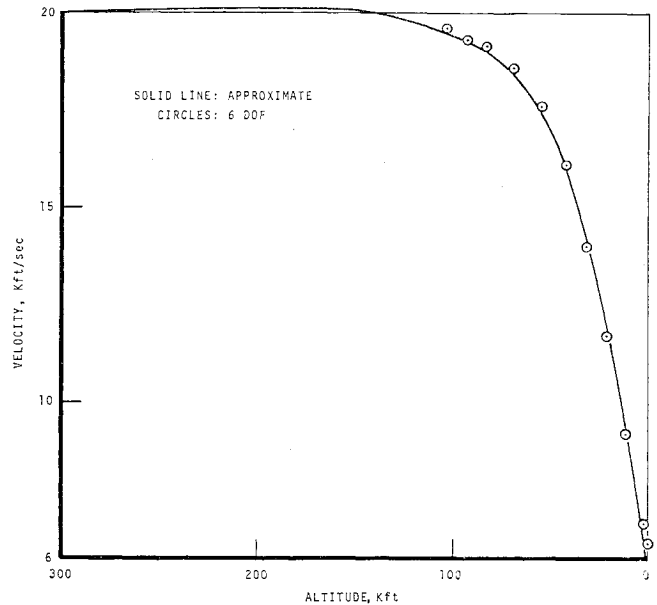


Fig. 2 Comparison of the total velocity obtained from the present analysis with that calculated using a 6-DOF program.

mately averages out. Hence, C_D is taken as

$$C_D = C_{D0} + C_{N\alpha} \left(\frac{\rho_e + a^2p^2}{\rho + a^2p^2} \right)^{1/2} \left[\left| \delta_e - \frac{I\dot{\xi}_e}{I_x p} \right|^2 e^{-2\Lambda_1} + \left| \frac{I\dot{\xi}_e}{pI_x} \right|^2 e^{-2\Lambda_2} \right] \quad (12)$$

The velocity is given by

$$m dV/dt = -\frac{1}{2} A \rho V^2 C_D + mg \sin \gamma \quad (13)$$

Assuming an exponential atmosphere, and changing variables in Eq. (13) give

$$dV^2/d\rho = -(AkC_D/m \sin \gamma) V^2 + 2gk/\rho \quad (14)$$

For a straight line trajectory (i.e., $\gamma = \text{const}$), Eq. (14) can be integrated to give

$$V^2 = V_e^2 e^{-f(\rho)} + 2k \int_{\rho_e}^{\rho} \frac{g}{\rho} e^{-f(\rho)} d\rho \quad (15)$$

where

$$f(\rho) = \frac{Ak}{m \sin \gamma} \int_{\rho_e}^{\rho} C_D d\rho \quad (16)$$

Substituting for C_D from Eq. (12) into Eq. (16), and performing the integration gives

$$f(\rho) = (AkC_{D0}/m \sin \gamma)(\rho - \rho_e) + (AkC_{N\alpha}/m \sin \gamma) \times \xi_e(\pi/2b_1)^{1/2} \exp(2b_1\rho_e + 2b_1a^2p^2 + s^2) \times \{ |\delta_e - I\dot{\xi}_e/I_x p|^2 \exp(4b_2ap\xi_e) [\text{erf}(\tau + s) - \text{erf}(\tau_e + s)] + |I\dot{\xi}_e/I_x p|^2 \exp(-4b_2ap\xi_e) [\text{erf}(\tau - s) - \text{erf}(\tau_e - s)] \} \quad (17)$$

where $\tau^2 = 2b_1(\rho + a^2p^2)$, and $s = b_2ap(2/b_1)^{1/2}$.

Figure 2 shows the good agreement between the velocity calculated from Eqs. (15) and (17) with that calculated using a six-degree-of-freedom computer program for $p = 50$ rad/sec. The calculations were done for the same body and trajectory parameters given at the end of the previous section.

4. Summary

An expression is given for the angle of attack of a high-performance entry body. This expression is shown to agree

with six-degree-of-freedom numerical solutions for widely varying roll rates. The angle-of-attack expression is used to calculate the drag, and the drag in turn is used to obtain an expression for the body velocity. The approximate solution for the velocity is in good agreement with a six-degree-of-freedom numerical solution.

References

- ¹ Allen, H. J. and Eggers, A. J., "A Study of the Motion and Aerodynamic Heating of Ballistic Missiles Entering the Earth Atmosphere at High Supersonic Speeds," Rept. 1381, 1958, NACA.
- ² Leon, H. I., "Angle of Attack Convergence of a Spinning Missile Descending Through the Atmosphere," *Journal of the Aerospace Sciences*, Vol. 25, No. 8, 1958, pp. 480-484.
- ³ Garber, T. B., "On the Rotational Motion of a Body Re-Entering the Atmosphere," *Journal of the Aerospace Sciences*, Vol. 26, No. 7, 1959, pp. 443-449.
- ⁴ Coakley, T. J., "Dynamic Stability of Symmetric Spinning Missiles," *AIAA Journal*, Vol. 5, No. 10, Oct. 1968, pp. 1231-1232.
- ⁵ Jaffe, P., "Terminal Dynamics of Atmospheric Entry Capsules," *AIAA Journal*, Vol. 7, No. 6, June 1969, pp. 1157-1158.
- ⁶ Nayfeh, A. H., "A Multiple Time Scaling Analysis of Re-entry Body Roll Dynamics," *Transactions of the Third Technical Workshop on Dynamic Stability Problems*, NASA Ames Research Center, Nov. 1968; also *AIAA Journal*, Vol. 7, No. 11, Nov. 1969, pp. 2155-2157.
- ⁷ Platus, D. H., "Angle-of-Attack Convergence and Windward-Meridian Rotation Rate of Rolling Re-Entry Vehicles," *Transactions of the Third Technical Workshop on Dynamic Stability Problems*, NASA Ames Research Center, Nov. 1968; also *AIAA Journal*, Vol. 7, No. 12, Dec. 1969, pp. 2324-2330.
- ⁸ "Equilibrium Roll Rate Theory for a Re-entry Vehicle," Document 67SD234, 1967, General Electric Co.

Ignition Catalysts for Furfuryl Alcohol—Red Fuming Nitric Acid Bipropellant

N. L. MUNJAL*

Birla Institute of Technology, Mesra, Ranchi, India

Introduction

THE hypergolicity of liquid propellants is a desirable characteristic because it eliminates the need for complex mechanical and electrical starting devices in rocket motors. It is not enough that the bipropellant be self-igniting; it is essential that it should have short ignition delay with smooth burning. This is necessary in order to prevent accumulation of dangerous quantities of unburned propellants in the combustion chamber. From this point of view, many investigations^{1,2} have been made to discover catalysts which could reduce the ignition delay of hypergolic propellants and improve the ignitability. The importance of discovery of catalysts is quite well known; sometimes the ignition of nonhypergolic propellants has been accomplished in the presence of certain catalysts.³⁻⁵

With these points in view, studies have been carried out to discover catalysts which could reduce the ignition delay of

furfuryl alcohol—red fuming nitric acid hypergolic bipropellant.

Materials

Red fuming nitric acid containing 16% water by volume was used as oxidant. Chemically pure furfuryl alcohol was used as such without any further purification. The following catalysts were used: a) soluble: potassium chromate, sodium nitroprusside, ferric chloride, zinc oxide, copper chromate, and magnesium powder; b) insoluble: ammonium metavanadate, sodium metavanadate, cuprous oxide, potassium dichromate, potassium ferrocyanide, cupric oxide, and potassium permanganate.

Measurement of ignition delay

The ignition delay (I.D.) was measured by cup test experiments, as described earlier.¹ First the catalyst was added in red fuming nitric acid containing 16% water by volume. The purpose of diluting red fuming nitric acid with water was to increase the ignition delay of furfuryl alcohol and the red fuming nitric acid (RFNA) system, otherwise the effect of catalysts would not have become apparent because the ignition of furfuryl alcohol with concentrated RFNA is almost instantaneous. It may also be mentioned here that NH_4VO_3 and Cu_2O which are known to be soluble catalysts¹ in RFNA, become insoluble in diluted red fuming nitric acid. Ignition delay was always measured by reacting 0.45 mliters of furfuryl alcohol and 0.60 mliters of the oxidant. The concentration of catalyst was 3 g in 100 cm^3 of RFNA. In certain cases, when the catalyst was insoluble in RFNA, the solution (RFNA + catalyst) was thoroughly shaken before use. The experiments were done at room temperature ($28 \pm 1^\circ\text{C}$).

Results and Discussion

The experimental results are given in Tables 1 and 2. From a practical view point and for convenience, soluble catalysts are preferred in injection, hence greater emphasis was placed on discovering these catalysts. Out of the soluble catalysts tried, potassium chromate, sodium nitroprusside, ferric chloride, zinc oxide, and copper chromate have been found to reduce the ignition delay of furfuryl alcohol-RFNA bipropellant (Table 1). But potassium chromate and copper chromate are the most effective in reducing the ignition delay and in both these cases very vigorous, smooth and elongated flames were observed. Of all the insoluble catalysts studied, ammonium and sodium metavanadates, cuprous oxide, potassium dichromate, potassium ferrocyanide, cupric oxide, and potassium permanganate reduce the ignition delay (Table 2). But it is noteworthy that sodium metavanadate, potassium dichromate, potassium ferrocyanide, and potassium permanganate reduce the ignition delay enormously and in case of these catalysts, very vigorous flames were observed. It may be mentioned here that in case of KMnO_4 catalyst, the fresh solution is always to be used otherwise it would lose its activity. The cause of this behavior has already been investigated by Rastogi and co-workers.⁵

The chemical rate processes occurring either during ignition or during steady-state combustion are not understood well enough to provide a complete explanation for the role of catalysts during ignition. The search for a suitable catalyst

Table 1 Average ignition delay in case of soluble catalysts

Catalyst	I.D., sec
None	1.8
Zinc oxide	1.1
Magnesium powder	1.1
Ferric chloride	0.8
Sodium nitroprusside	0.7
Potassium chromate	0.4
Copper chromate	0.35

Received August 19, 1969; revision received November 14, 1969. The author wishes to thank G. B. Pant, Head of the Department of Space Engineering and Rocketry for his interest in this investigation. Thanks are due to the Aeronautical Research Committee of Council of Scientific and Industrial Research, New Delhi for financial support.

* Associate Professor, Propellant Chemistry Section, Department of Space Engineering and Rocketry.